Leskinen, Timo; Witos, Joanna; Valle-Delgado, Juan José; Lintinen, Kalle; Kostiainen, Mauri; Wiedmer, Susanne K.; Österberg, Monika; Mattinen, Maija Liisa

Adsorption of Proteins on Colloidal Lignin Particles for Advanced Biomaterials

Published in:
Biomacromolecules

DOI:
10.1021/acs.biomac.7b00676

Published: 11/09/2017

Document Version
Peer-reviewed accepted author manuscript, also known as Final accepted manuscript or Post-print

Adsorption of proteins on colloidal lignin particles for advanced biomaterials

Timo Leskinen[1], Joanna Witos[3], Juan José Valle-Delgado[1], Kalle Lintinen[2],Mauri Kostiainen[2], Susanne K. Wiedmer[3], Monika Österberg[1], and Maija-Liisa Mattinen[1]*

1. Bioproduct Chemistry, Department of Bioproducts and Biosystems (Bio^2), Aalto University, P.O. Box 16300, FI-00076 Aalto, Espoo, Finland
2. Biohybrid Materials, Department of Bioproducts and Biosystems (Bio^2), Aalto University, P.O. Box 16300, FI-00076 Aalto, Espoo, Finland
3. University of Helsinki, Department of Chemistry, A.I. Virtasen aukio 1, P. O. Box 55, 00014 University of Helsinki, Finland

Abstract

Coating of colloidal lignin particles (CLPs), or lignin nanoparticles (LNPs), with proteins was investigated in order to establish a safe, self-assembly-mediated modification technique to tune their surface chemistry. Gelatin and poly- L-lysine formed the most pronounced protein corona on the CLP surface, as determined by dynamic light scattering (DLS) and zeta potential measurements. Spherical morphology of individual protein coated CLPs was confirmed by transmission electron (TEM) and atomic force (AFM) microscopy. A mechanistic adsorption study with several random coiled and globular model proteins was carried out using quartz crystal microbalance with dissipation monitoring (QCM-D). The three-dimensional (3D) protein fold structure and certain amino acid interactions were highly dependent on the protein adsorption on the lignin surface. The main driving forces of protein-lignin affinity were electrostatic, hydrophobic, and Van der Waals interactions, and hydrogen bonding. The relative contributions of these interactions were highly dependent on the ionic strength of the surrounding medium. Capillary electrophoresis (CE) and Fourier transform infrared spectroscopy (FTIR) provided further evidence about the adsorption-enhancing role of specific amino acid residues such as serine and proline. These results have high impact on the utilization of lignin as colloidal particles in

biomedicine and biodegradable materials, as the protein corona enables tailoring of the CLP surface chemistry for intended applications.

KEYWORDS: colloidal lignin particle (CLP), lignin nanoparticle (LNP), protein, corona, self-assembly, quartz crystal microbalance with dissipation monitoring (QCM-D)

Introduction

Lignin has versatile attributes as an aromatic, antioxidative, and antimicrobial biopolymer. Conversion of industrially isolated lignins into soft submicron sized colloids provides an attractive new way for valorization of the underutilized lignin biopolymer, as recently reviewed by Zhao et al. (2016)[1]. These colloids can vary in size from below 100 nm to several hundred nanometers and in general from stabile aqueous dispersions. These colloidal particles are referred to as lignin nanoparticles (LNPs) or, as here, colloidal lignin particle (CLPs). Owing to the colloidal properties, the CLP technology is presupposed to find its way to industrial sectors that produce bulk products like adhesives and composites.[2] In addition to these high-volume applications, biologically compatible CLPs[3] carry potential for advanced biomedical applications, including microencapsulation of active compounds[4,5] or injectable hydrogels thereof[6], formulations for tissue repairing[7], and wound dressings[8].

Recent studies[4,9–14] have described the preparation of nanosized lignin particles, which are stabile in aqueous dispersions. Formation of CLPs using the solvent exchange method[10,12–14] is driven by lignin self-assembly *via* interpolymeric, majorly π-electron mediated, interactions when the lignin-solvation capacity of the medium is reduced. The current view is that hydrophobic functional groups form the core of single CLPs while hydrophilic groups such as hydroxyl of carboxylic acid groups more favorably locate on the outer shell of the particles.[10,12–14] Hence the stability of individual CLPs in aqueous dispersions is obtained *via* negative surface charge arising from the orientation of ionizable functional groups towards the particle surface.[12–14]

In order to control interactions and compatibility of CLPs with physiological environment, or any components within a variety of biomaterials, the surface chemistry of the particles often requires

modification. Covalent chemical modification of lignin surfaces does not offer such safe reagent free alternatives. Limited studies exist on a self-assembly driven mechanism to coat CLP surfaces by synthetic polycations like poly(diallyldimethylammonium chloride) (PDADMAC).[12,14–15] Proteins, as natural and biocompatible polymers, are interesting alternatives to the synthetic polymers for CLP surface modification, due to the related safety aspect. In medical applications, even proteins from the patient's own body could be utilized for coating.

Recent research on various types of lignin model films has shown that proteins and peptides adsorb easily on lignin surfaces.[16–20] Still, proteins are complex 3D-structured molecules and fundamental knowledge on amino acid specific interactions and influence of protein fold structures on their interaction with the lignin surface remains limited. Aromatic and charged amino acid side-chains of a specific flat face of cellulose binding modules (CBMs) of cellulases[16,18,19], are essential for lignin interactions, as confirmed by studying different amino-acid mutations on the binding face. Recently, Yamaguchi et al. (2016)[20] have shown the importance of various amino acid side-chains on lignin interactions using synthetic 12-mers. Peptides containing histidine, phenylalanine, proline, and serine residues had the best affinity to the lignin surface. Furthermore, the botanical origin of lignin was shown to affect peptide-lignin interactions. Besides a number of potentially interacting amino acid side-chains within a protein fold, alteration of their accessibility by denaturation influences proteins adsorption on lignin surfaces.[17]

Better understanding of lignin-protein interactions is required in order to utilize CLPs in advanced bionanomaterial applications involving proteins. Whether the protein adsorption on different surfaces is driven by specific (e.g. ion pairing or hydrogen bonding) or non-specific mechanisms, such as hydrophobic driving force, is under debate.[21] Penna et al. (2014)[22] proposed that protein adsorption on hydrated surfaces occurs in different stages, in a way that an initial weak contact between the protein and the surface lead to a "statistical zippering" effect, mediated by strongly interacting amino acid side-chains. Thus, fundamental investigation of interactions in protein-CLP systems, and between proteins and biomaterial surfaces in general, is essential.

In this contribution, we introduce the formation of protein corona on CLPs *via* adsorption-driven assembly process. Several globular and random coil proteins and peptides were studied for this purpose in aqueous media. Besides formation of protein corona on CLPs, fundamental

mechanisms behind adsorption of structurally and chemically different proteins on lignin were studied by advanced analytical techniques. This approach allowed for identifying several structural and compositional key factors affecting protein adsorption on the CLP surface. The results contribute strongly to the applicability of the particles to advanced biomaterial applications in medicine, cosmetic, and food sectors. The mechanistic studies aim to contribute to the development of general models of protein interaction with structurally heterogeneous biomaterial surfaces (i.e. defining the interplay between protein structure and amino acid composition).

Experimental

Materials. Solvents, model proteins, and all other chemicals were reagent grade and they were ordered from Sigma-Aldrich (Finland) or Fisher Scientific (Finland). Gelatin was purified using dialysis (21 kDa cut-off) and freeze dried prior to use. Softwood Kraft lignin LignoBoost™ from Valmet (Finland) was used to prepare CLPs according to Lievonen et al. (2015).[12] In addition to the original procedure, the CLP dispersion was centrifuged at 5000 – 9000 rpm to remove possible aggregated CLPs. For the FTIR experiments, the CLP samples were further purified after protein addition by diafiltration in Amicon 8200 stirred cell (Merck Millipore, Germany) using polyethersulfone-coated polyethylene/polypropylene (PE/PP) membrane (150 kDa cut-off). In the case of the experiment shown in Figure 2B, further syringe filtration (220 nm pore size) was applied after 9000 rpm centrifugation and membrane purification.

Table 1. Properties of peptides and proteins used in the study, provided by suppliers and reference literature listed in the Supporting Information.

	Gelatin	**Casein**	**Bovine serum**	**Conalbumin**	**Albumin**
Mw (kDa)	47	19 – 24	-	76	66
pI	7.0 – 9.0	4.1 – 5.8	-	6.8	4.8 – 5.6
Amino acid composition					
Positive (wt.%)	12	12	-	17	17
Negative (wt.%)	15	28	-	23	25

Polar (wt.%)	17	10	-	10	9
Hydrophobic (wt.%)	19	39	-	37	36
Cys, Pro, Gly (wt.%)	36	7	-	11	10
3D structure	No	No	Yes	Yes	Yes
Solubility in water	Good at 40°C	Poor	Good	Good	Good

Adsorption of proteins on lignin thin films. The lignin thin films were prepared on gold coated QCM-crystals (Q-Sense, Sweden) as described by Salas et al. (2012)[17] except that the concentration of lignin in dioxane-water (82:18 v/v) solution was 0.5 mg/mL. The spin-coating sequence was 300 rpm (3 s), 1000 rpm (5 s), and finally 2000 rpm (30 s). Polystyrene (PS) and polyethylene (PE) films (four layers) were spin coated from toluene solutions. AFM images and water contact angle measurements of the films are shown in the Supporting Information (**Figure SI1** and **Table SI1**).

Adsorption of proteins on the thin films were carried out using QCM-D E4 (Q-Sense, Sweden) in continuous flow mode. Proteins were dissolved (10 μg/mL) in phosphate buffered saline (PBS) at pH 7.4 and ionic strength of 0.18 M at ambient temperature. Mixing (1 h) at 40 °C was applied for gelatin and casein mixture due to slow solubility at ambient temperature. The more soluble sodium caseinate form of this protein was used in case of the DI water medium and adsorption of proteins on PE films. During the QCM-D measurements, lignin films were exposed to protein solutions using a 0.1 mL/min flow rate at 25 °C and subjecting films to protein adsorption under the same flow rate for 30 min. In the case of poly-L-lysine anchoring, the poly-peptide layer was first formed inside the QCM-D chamber as described above. After protein adsorption, the films were rinsed with buffer for 30 minutes (45 min in the case of poly-L-lysine). Masses of the adsorbed protein films, including bound water, were calculated from observed frequency changes using a method developed by Johannsmann (1992).

Coating CLPs with proteins. CLP dispersion (2 mL, 0.1 mg/mL, pH 4.3) and protein solutions (0.35 mL) were mixed in a 4 mL vial and left to stabilize overnight prior to the measurement. Protein to lignin mass ratios (10 to 0.002) were adjusted by dilution of the added protein solutions.

Average particle sizes and electrophoretic mobilities were measured by Zetasizer (Nano-ZS90). For FTIR samples, the procedure was carried out in 30 mL scale.

Particle size and zeta potential measurements. A Nano-ZS90 Zetasizer from Malvern, UK, was used to measure average particle sizes and zeta potentials. A dip cell probe was used for the electrophoretic mobility measurements, which were used to obtain the zeta potentials. All experiments were performed with triplicate samples. Three scans were recorded for zeta potential and two for particle size measurement. Intensity based average particle sizes and zeta potential values of the CLP dispersions varied between 210 to 230 nm and -30 to -42 mV, respectively.

Capillary electrophoresis. CE analysis to study the influence of CLPs on amino acid mobilities was performed using an Agilent 7100 CE system (Agilent Technologies, USA) equipped with a UV-Vis diode-array detector. The background electrolyte solution comprised 20 mM sodium benzoate at pH 9.0 without (control samples) or with 25 vol.% of lignin particle dispersion (0.1 mg/mL). The concentrations of the amino acids in the sample for injection were 0.5 – 1.0 mM (in water). Thiourea with a concentration of 0.5 mM was used as the electro-osmotic flow marker. The total length of the fused silica capillary with a 50 μm inside diameter and a 360 μm outside diameter (Polymicro Technologies, USA) was 38.5 cm, with a length of 30.0 cm to the detector. A separation voltage of 25 kV and sample injection for 6 s at 50 mbar were used for the analyses.

FTIR spectroscopy. Coated CLPs were freeze dried after preparation and all samples were dried in vacuum oven for 20 h at 25 °C. FTIR spectra were recorded using Thermo Nicolet iS50 FTIR spectrometer with iS50 ATR-crystal (Thermo Fisher scientific, USA). Analysis from the spectral area (3800 - 600 cm^{-1}) was carried out as duplicate measurements with 32 scans each, and all collected spectra were averaged prior normalization. Area normalization was applied to the final spectra using Excel (Microsoft, USA).

Microscopic analyses. The AFM analyses were carried out with a MultiMode 8 atomic force microscope equipped with a NanoScope V controller (Bruker Corporation, USA), operating in tapping mode. The images were obtained in ambient air with NCHV-A tapping mode probes from Bruker. Research NanoScope 8.15 software (Bruker, USA) was used for image analysis. The only

image correction applied was flattening. TEM analyses were carried out as described by Lievonen et al. (2015)[12] with exception that porous grids were used.

Analysis of protein structures. Crystal structure conalbumin[23] (PDB ID: 2D3I) was obtained from RCSB-protein databank (http://www.rcsb.org/). Downloaded structure was processed with Chimera-software (version 1.11) (UCSF, USA).[24] Average values for amino acid compositions were calculated from several literature sources (see Supporting Information for references, section **SI3**). Amino acid compositions (wt.-%) were plotted against the sensed mass of adsorbed proteins from QCM-D experiments using Excel software. Correlation factors (r^2), describing the interrelation between the abundance of a specific amino acid and the adsorption of proteins, were determined using linear trendline functions.

Results and discussion

Functionalization of CLP surfaces *via* protein self-assembly. Coating of CLP surfaces with different proteins *via* self-assembly was studied in aqueous media at pH 4.3 without added salts. Peptides poly-L-lysine or poly-L-proline, or physiologically relevant proteins (gelatin and serum) were added individually into the dispersions and changes in the average particle sizes and zeta potential values were determined as a function of protein concentration (**Figures 1** and **2**, see also Supporting Information **Figures SI2** and **SI3**).

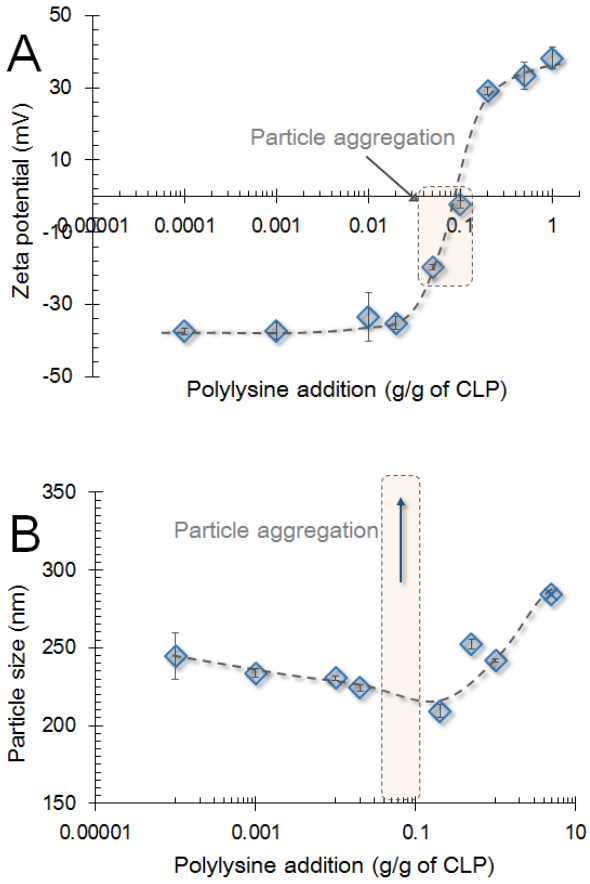

Figure 1. (A) Zeta potential values and **(B)** particle size distributions of CLPs after coating with varying amounts of poly-L-lysine peptide.

The adsorption of highly positively charged poly-L-lysine onto the negatively charged CLPs was evident from the reversal of the surface potential upon polypeptide corona formation (**Figure 1 A**), with a concomitant increase in the average particle size (**Figure 1 B**). Upon addition of poly-

L-lysine to the CLP dispersion, a loss of colloidal stability and subsequent aggregation of the particles occurred when the surface charge was close to zero, i.e. at 0.1 g/g of poly-L-lysine/CLP concentration. The behavior was very similar to the adsorption of synthetic polyelectrolytes observed earlier.[12] When using poly-L-proline that has neutral cyclic amino acid side-chains, the corona formation did not lead to charge reversal, and thus it was more challenging to verify the adsorption. **Figure SI3** shows that here was a ca. 10 nm increase in the particle size as well as a weak reduction in the electrophoretic mobility when poly-L-proline was introduced, providing some indication about its adsorption onto the CLPs. It seems that even non-Coulombic interactions, such as hydrogen bonding of amide backbone or even interactions mediated by π-electrons of aromatic groups in lignin and -CH_2- of the proline ring, [25,26] may drive adsorption of the neutral poly-L-proline on lignin surface to some extent, sufficiently enough for corona formation.

A pronounced protein corona was also formed with the positively charged gelatin protein (**Figure 2 A** and **B**). In contrast, adsorption of mixtures of different globular serum proteins (**Figure SI3**) or negatively charged random coil caseins on CLP surface from unbuffered medium where charge repulsion took place, could not be verified using light scattering methods. Even so, some amounts of these proteins were detected from purified CLP samples by MALDI-TOF and QCM-D analyses, suggesting a small amount of adsorbed proteins (Supporting Information **Figure SI4** and **Table SI3**). The adsorption of gelatin on the CLP surface was evidenced by a ca. 70 nm increase in the average particle size (**Figure 2 A** and **B**). The net surface charge of the gelatin coated CLPs remained slightly negative (**Figure 2 C**), regardless of the weak positive net charge of the adsorbed protein. Thus, we conclude that a high positive charge density of adsorbing protein species is required for complete charge reversal of CLPs, as was the case with poly-L-lysine.

Formation of the gelatin corona on the CLP surface was further confirmed by FTIR spectroscopy (**Figure 2 D**) by the presence of characteristic amide bands. Microscopic analyses by AFM and TEM (**Figure 2 E** and **F**) showed the presence of single CLPs, but no visible changes in the surface morphology in comparison to uncoated CLPs (Supporting Information **Figure SI5**). However, microscopic analyses of dispersions dried on sample plates showed clearly the formation of aggregates where the soft gelatin coating seemed to act as an adhesive layer between particles (**Figure 2 E** and **F**).

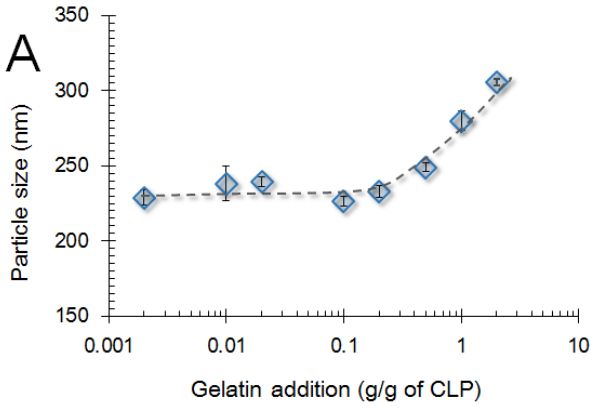
A
350
300
250
200
150
Particle size (nm)
0.001
0.01
0.1
1
10
Gelatin addition (g/g of CLP)

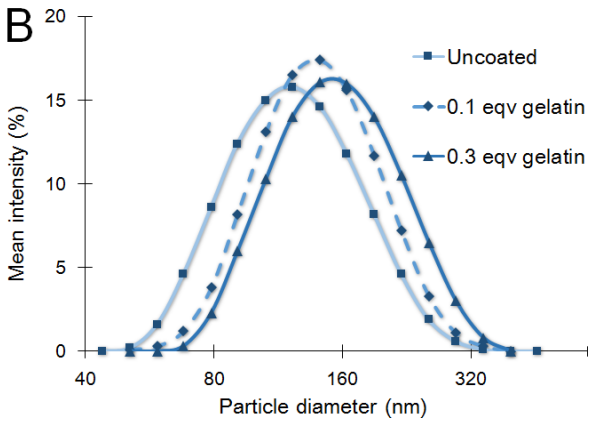
B
20
15
10
5
0
Mean intensity (%)
Uncoated
0.1 eqv gelatin
0.3 eqv gelatin
40
80
160
320
Particle diameter (nm)

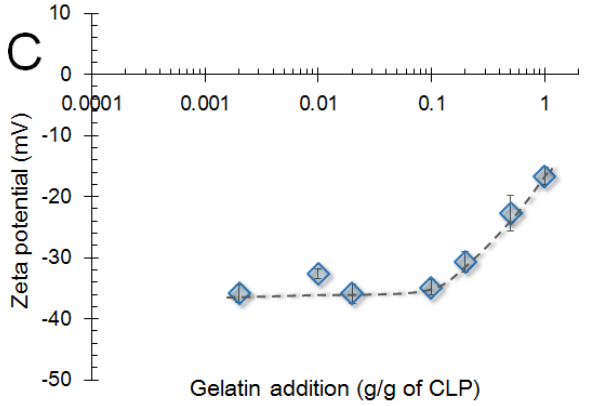
C
10
0
-10
-20
-30
-40
-50
Zeta potential (mV)
0.0001
0.001
0.01
0.1
1
Gelatin addition (g/g of CLP)

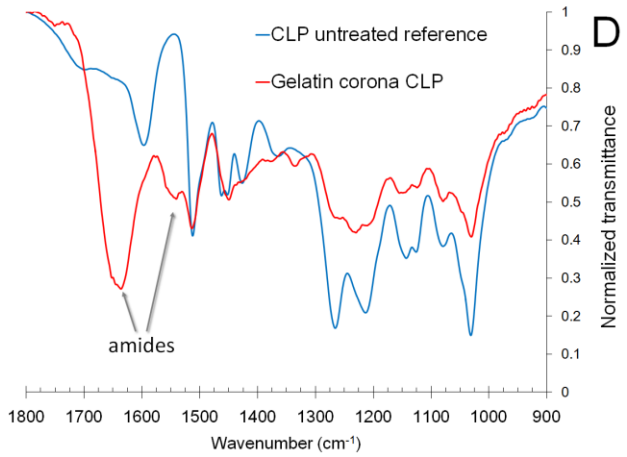

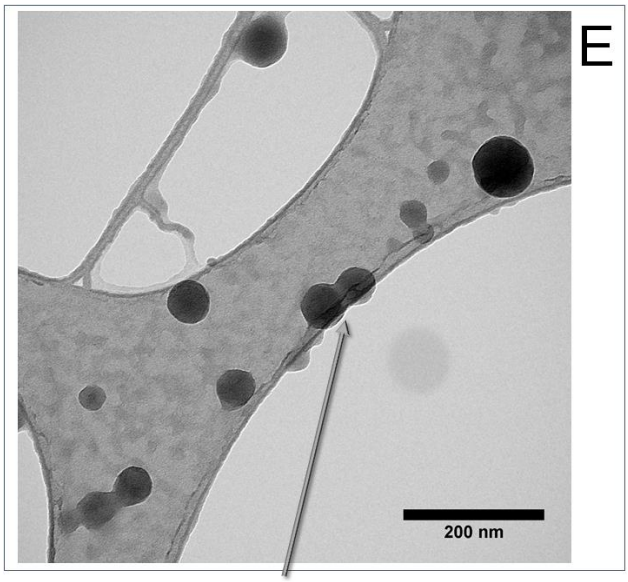

Adhesion of CLP via gelatin corona upon drying

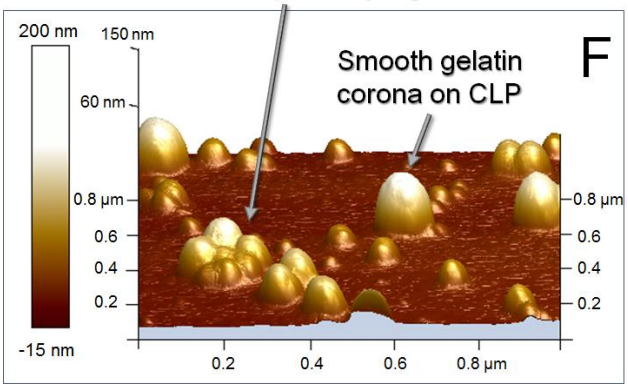

Figure 2. Formation of gelatin corona on CLPs. **(A)** Average particle sizes, **(B)** shift in the particle side distribution, and **(C)** seta potential values of CLPs as a function of protein concentration. **(D)** FTIR-spectrum of gelatin coated CLPs after 1 wt. eqv protein addition. (**E**) TEM image after 0.3 wt. eqv protein addition and **(F)** AFM image after 0.3 wt. eqv protein addition. Trendlines in A and C are drawn only for aiding the visualization of the data.

Our results show, that in a very low ionic strength medium proteins and peptides bearing positive net charge are potential biopolymers for corona formation on CLP surface. In high ionic strength medium, where repulsion between negatively charged proteins and negatively charged CPL surface can be screened out, the interactions between proteins and lignin surface are more complex, allowing interactions also *via* non-ionic mechanisms (see next chapter). Adsorption of weakly charged proteins and peptides, such as gelatin or poly- L-proline, is interesting regarding potential medical applications.

Adsorption of proteins on lignin films. A mechanistic study of protein-lignin interactions was carried out by QCM-D using lignin films, having the same starting materials as the CLPs. Although the surface roughness of spin coated lignin thin films is usually low when a good solvent is used,[17,25] the AFM images of lignin films spin-coated from dioxane-water revealed that the surface structure of our films consisted of ca. 50 nm spherical lignin structures (**Figure SI1**). The dioxane-water mixture used for thin film preparation thus produced a corresponding aggregation effect that occurs during CLP formation.[13] Hence these films are ideal model surfaces for CLPs.

Globular albumin and conalbumin, random coil casein mixture and gelatin, and a mixture of serum proteins were used as model proteins (**Table 1**) to investigate the main protein properties governing the adsorption onto lignin. **Figure 3** shows the sensed mass upon protein adsorption at high ionic strength 180 mM phosphate buffered saline (PBS), resembling the physiological environment of biomedical applications. The sensed masses measured for adsorbed protein films were significantly different depending on the physico-chemical properties of the proteins (**Table 1**). All proteins adsorbed to some extent, but gelatin, casein and bovine serum showed clearly the highest sensed mass, while albumin and conalbumin adsorbed considerably less, and the slow kinetics for albumin adsorption suggests low affinity to lignin. As such the most significant

differentiating factor between proteins was their random coiled or globular structure. It is noteworthy that a high sensed mass was even found for net negatively charged casein, illustrating that at high ionic strength the double layer repulsion between negatively charged lignin and negatively charged protein is sufficiently short-ranged to be overcome by other attractive forces. Some differences were detected in the viscoelastic properties of protein layers during the adsorption processes (Supporting Information **Figure SI6**), indicating that globular protein films may be less swollen or have a more packed organization. Regardless that the hydration and swelling behavior of these protein films in the applied medium cannot be expected to be identical, the observed differences clearly exceeded typical variances in the degree of bound water or swelling of protein films, which depends on the type of protein or its denaturation.[17]

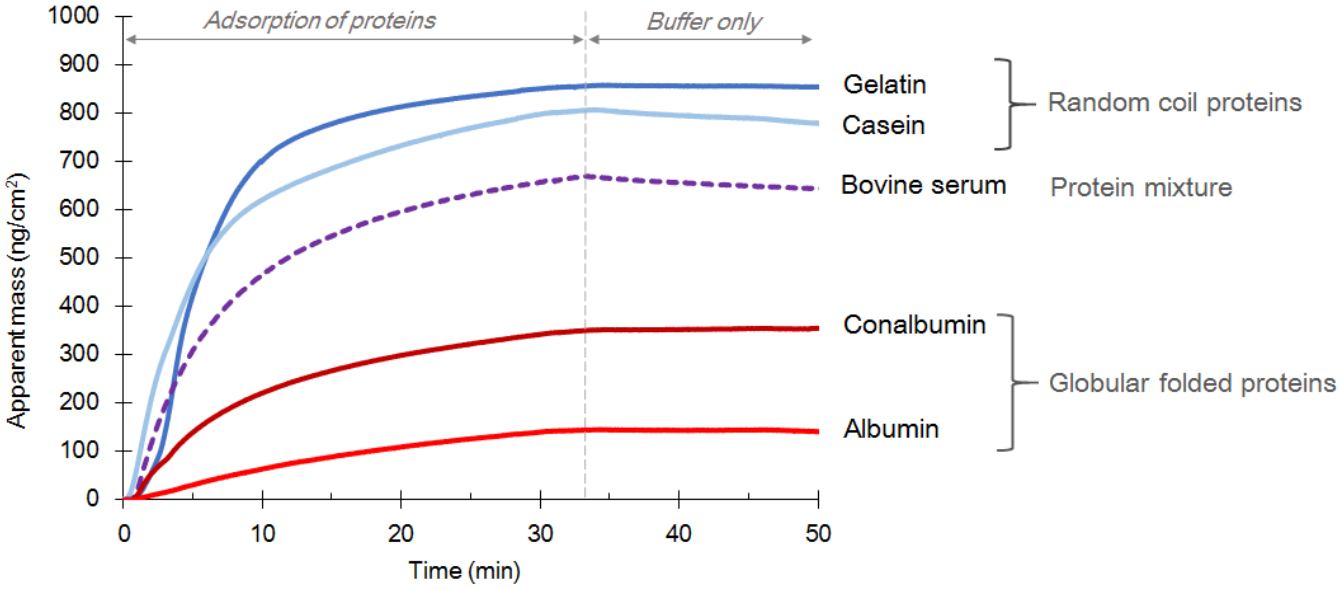

	Gelatin	Casein	Bovine serum	Conalbumin	Albumin
Adsorption on lignin film (apparent mass, ng/cm²)	824 ± 49	767 ± 65	672 ± 6	331 ± 49	155 ± 35

Figure 3. Effect of protein structure on the adsorption on lignin thin films as analyzed by QCM-D in PBS buffer solution with ionic strength of 180 mM.

Cooperativity of protein adsorption on particles has been reported previously[28], however, further investigation of such phenomenon, and thus further mechanistic studies with serum proteins, is out of the scope of this study. Yet the influence of cooperative adsorption seems evident as mixtures

of globular and random coil proteins (bovine serum) adsorbed readily on lignin surface, while the globular bovine serum albumin showed the weakest adsorption on lignin thin film.

Effect of protein 3D structure on the adsorption. In addition to the 3D structure, flexibility of the peptide backbone is affecting protein adsorption on solid surfaces.[29] Unfolding of the protein's 3D structure allows conformation adjustment in respect to solid surfaces, thus enhancing the adsorption process via the "statistical zippering" mechanism[22] Denaturation has been shown to improve adsorption of globular proteins on hydrophobic surfaces,[17,29] while surprisingly an opposite effect has also been reported in the case of lignin surfaces.[17] To avoid e.g. possible competitive interactions of denaturing agents with the lignin surface, naturally globular and random coiled proteins were applied in this study.

As shown in **Figure 3**, adsorption of random coil gelatin and casein was the strongest on the lignin thin films. Looking at the protein compositions at amino acid residue level and correlating this with the observed adsorption of the proteins provided further rationale for such observation, as an inverse correlation was seen between the number of cysteine residues and the mass of the adsorbed protein layer (**Table 2**). Disulfide bridges formed by cysteine pairs are known to stabilize folds of globular proteins[30] such as albumin and conalbumin, while random coil proteins lack these structures. Our results support the view that the flexibility of protein folds is highly beneficial for establishment of favorable non-covalent interactions with the lignin surface during the adsorption process of proteins.

Table 2. Correlation (r^2) between amino acid composition of the model proteins and extent of adsorption onto lignin surface in PBS medium (180 mM).

Residue / group	**Amino acid composition** (wt. %)				**Correlation to lignin adsorption** (r^2)
General groups	**Albumin**	**Casein**	**Conalbumin**	**Gelatin**	
Positively charged (R, H, K)	20	15	19	12	-0.94
Negatively charged (D, E)	25	28	23	15	-0.10
Polar (S, T, N, Q)	9.0	10	10	17	0.47
Hydrophobic (A, I, L, M, F, W, Y, V)	36	39	37	19	-0.23
Backbone (C, G, P)	9.6	13	11	36	0.46
Hydrophobic + backbone (A, I, L, M, F, W, Y, V, C, G, P)	46	52	48	54	**0.96**
–OH containing (Hyp, S, T, Y)	14	16	14	17	**0.89**
Cysteine (C)	3.7	0.4	3.1	0.0	**- 0.98**
Proline (P)	4.3	10	3.8	14	**0.86**
Residues with high lignin affinity[16,18–20]					
Histidine (H)	3.6	3.0	2.3	0.8	- 0.39
Phenylalanine (F)	6.0	5.2	4.8	2.1	- 0.47
Serine (S)	3.7	5.8	5.2	3.4	0.02
Tyrosine (Y)	4.7	5.7	4.1	0.5	- 0.16

Interplay of Coulombic interactions and ionic strength of the adsorption medium. Coulombic interactions are a fundamental driving force when polyelectrolytes such as proteins are adsorbed from low ionic strength solutions, but have less significance at high salt concentrations e.g. in physiological media, or in the case of adsorption towards strongly hydrophobic surfaces[21,29]. As the intended medical applications are based on use of strongly buffered medium, we investigated to what extent Coulombic interactions and screening thereof influences protein adsorption on CLPs.

CLPs and lignin thin films bear a negative charge at pH above 4,[9,12,14] which was expected to favor adsorption of positively charged proteins. **Figure 4** and **Table SI3** in supporting information show how protein adsorption on model lignin films was significantly, but not solely, determined by the net surface charge of the protein in the case of non-ionic medium, whereas high ionic strength of the applied medium diminished the influence of charge interactions.

In the case of positively charged gelatin (pI 7.0 – 9.0), the dependence of adsorption on the ionic strength of the media was clear, with the highest sensed mass observed in water and lowest in PBS. This suggest a dominance of attractive double layer forces as the sensed mass increased by 124 % from PBS to water (**Figure 4 A**). It is worth noting that the ionic strength of the medium seems to have a negligible effect on the coil conformation of gelatin and we see a purely negative effect of increasing the ionic strength on the sensed mass of the adsorbed protein layer. This is different to the typical swelling behavior of flexible random coil polyampholytes[31]. On the contrary, the adsorption of negatively charged casein (pI 4.1 – 5.8) was nearly diminished in a low ionic strength medium when no salt was present (**Table SI3**).

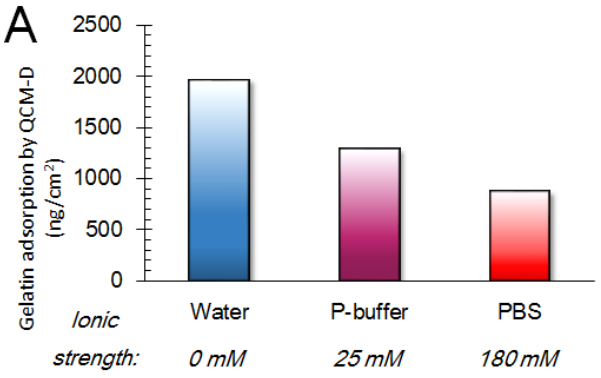

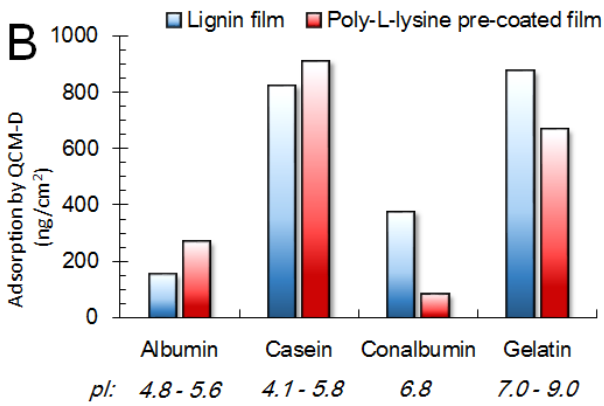

Figure 4. Experiments demonstrating the effect of Coulombic interactions and medium on protein adsorption on lignin surface as analyzed by QCM-D. **(A)** Adsorption of gelatin on lignin thin film from three different buffers with varying ionic strength. **(B)** Adsorption of four model proteins on lignin thin films from PBS medium, and alternatively on same lignin film after pre-coating with poly-L-lysine.

Pre-coating of negative lignin films with positively charged poly-L-lysine prior to injection of the model proteins was investigated (**Figure 4 B** and **Figure SI7**). Regardless of the charge screening effect by PBS, the negatively charged proteins had increased adsorption on the poly-L-lysine coated lignin film, indicating that charge attraction with the coating layer took place to some extent. The increase in adsorbed mass was ca. 43 % for albumin and ca. 11 % for casein. Accordingly, the cationic coating reduced the adsorption of the positively charged gelatin by ca. 24 %. Adsorption of conalbumin reduced ca. 78 %, while the charge of this protein was close to neutral or slightly negative at pH 7.4 of the PBS buffer, which emphasizes that the folded conformation or other interactions than Coulombic ones also strongly contribute to its adsorption on lignin surface.

In PBS the random coil proteins gelatin and casein had significantly higher adsorption on lignin surface compared to that of globular albumin and conalbumin, regardless of the pI of the proteins. Thus, the structural properties of proteins or non-charge mediated interactions have higher impact on lignin-protein interaction under charge screening conditions, even at the low ionic strength (25 mM) of PBS-buffer (supporting information).

Effect of hydrophobic interactions. Besides charge interactions, hydrophobic driving force is known to affect strongly the adsorption of proteins.[21,29,32] In the case of strongly hydrated surfaces the hydrogen bonding with hydration layer is the major initial interaction during the anchoring phase of protein adsorption.[22] Instead, when using poorly hydrated surfaces, such as PE films, alternative interactions are required for efficient protein adsorption.[29,32] Lignin is an interesting substrate as it is hydrated in aqueous medium due to presence of numerous hydroxyls on its surface, while hydrophobic interactions have also been proposed to contribute strongly to protein-lignin interaction e.g. in the case of cellulases[18].

Water solubility of a protein is somewhat analogous to its overall hydrophobicity and thus the affinity towards hydrophobic surfaces. The water solubility of the model proteins used in this study correlates inversely with their observed adsorption on lignin (**Table 1**), as the strongest adsorbing proteins, gelatin and casein, are also the least soluble in aqueous medium. Regardless of the seemingly evident interconnection to the knowingly very influential hydrophobic driving force[21,29,32], hydrophobicity alone does not explain the whole adsorption phenomenon of the tested model proteins on lignin films.

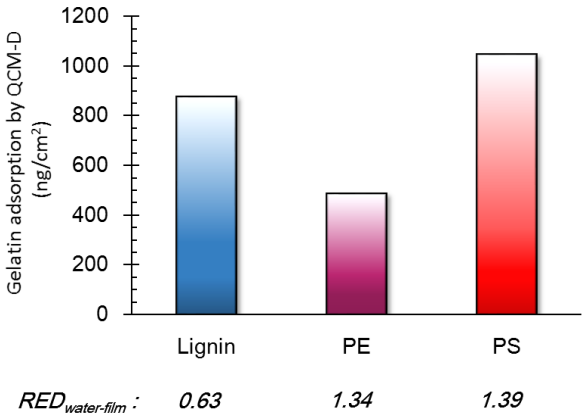

Figure 5. Gelatin adsorption on different films with varying hydrophobicity and surface functionality, as analyzed by QCM-D. Relative energy differences ($RED_{water - film)}$ were calculated using Hansen solubility parameters to indicate the relative hydrophobicity of the three films. For clearly hydrophobic films the RED value is > 1. (Section SI6 of the Supporting Information for more details).

The role of the hydrophobic driving force on gelatin adsorption on lignin film was evaluated by comparing gelatin adsorption to lignin surface with the adsorption to PS and PE films, as shown in **Figure 5**. The adsorption on the aliphatic hydrocarbon surface of PE film was expected to be mainly mediated by the hydrophobic force, without significant contribution from other than weak van der Waals interactions. The resulting adsorption of 490 ng/cm^2 indicates significant contribution of hydrophobic forces on the protein adsorption on PE-film, albeit the adsorbed amount is still the lowest among the three films. Employing another strongly hydrophobic PS film resulted in the highest (1050 ng/cm^2) observed gelatin adsorption. At the same time, for the rather hydrophilic lignin film the adsorption was only somewhat lower (880 ng/cm^2) than in the case of PS. The results indicate that besides purely hydrophobic driving force and Coulombic interactions, there are other types of interactions as well that strongly affect protein adsorption. On lignin and PS films, a common functional group is the aromatic ring and its π-electron system, which participates in multitude of polar interactions[25,26]. These interactions apparently contribute as strongly as the hydrophobic effect to the affinity of gelatin on lignin and PS.

Role of amino acid side-chains on the protein adsorption. It has been shown that certain amino acid side-chains interact strongly with lignin.[16,18–20] These amino acids and their abundancies in the studied model proteins are summarized in **Table 2**. Although adsorption of proteins and peptides on various surfaces can be predicted, at least to a certain extent, on the basis of amino acid sequence and/or composition,[20,33] no significant correlations between adsorption of the knowingly well interacting amino acid side-chains and lignin film were observed in this study. Especially for the class of globular proteins, this can be explained by the fact that most of the potentially interacting amino acid side-chains are typically located inside the 3D structure of the protein. Only a few of these residues with known lignin affinity are located on the surface of the protein, as demonstrated for conalbumin in **Figure 6**. For the class of random coil proteins as gelatin and casein, these amino acid side-chains are more accessible. Besides well-known amino acid lignin interactions, several other interesting correlations regarding potential residue types that may promote protein adsorption on lignin were discovered. Besides the above mentioned correlation to cysteine content, correlations were found to contents of hydrophobic residues in addition to so called backbone residues, side-chain hydroxyl containing residues, and quite surprisingly to proline, which are highlighted in the **Table 2**.

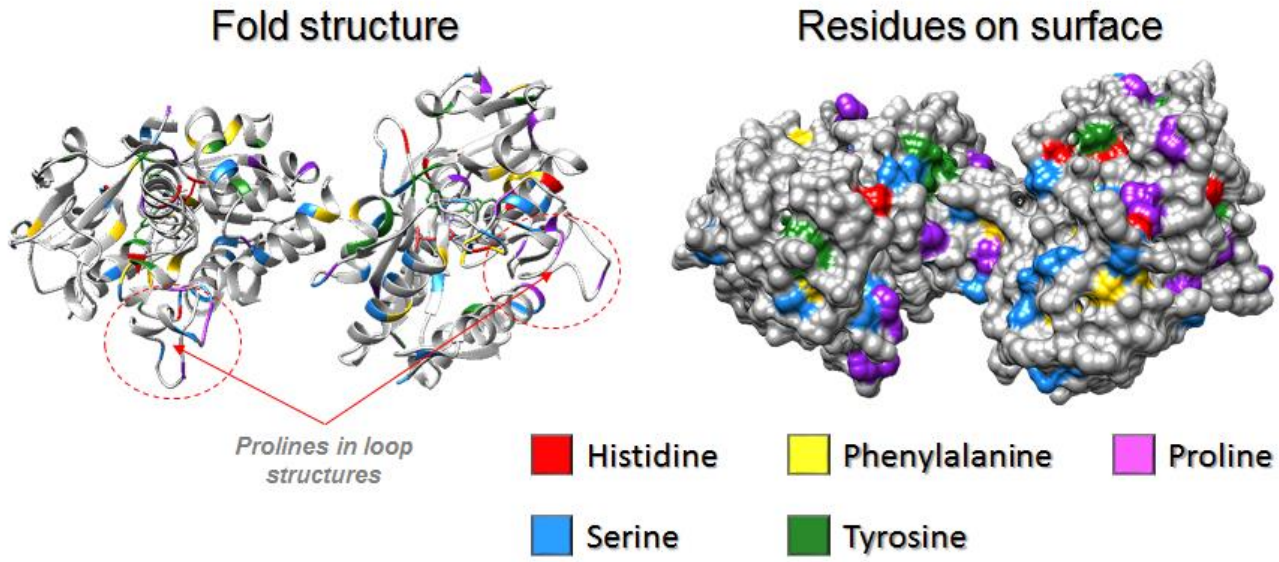

Figure 6. Selected amino acid residues highlighted on the surface of the folded Conalbumin (PDB ID: 2D3I) using Chimera™ software.

As expected, the amount of charged amino acids did not correlate with protein adsorption in PBS-buffer. The proposed hydrophobic interactions were not evident either based on the number of hydrophobic amino acid residues (r^2 = -0.23). However, when combined with the number of backbone residues, glycine and proline, a significant correlation (r^2 = 0.96) was found. The result is in agreement with data presented in this study regarding the effect of hydrophobic interactions. The side-chain of proline is an aliphatic hydrophobic ring, but when neighboring with a small glycine residue the flexibility of the protein backbone is increased[34,35], facilitating hydrophobic interactions of other amino acid side-chains. Yet, it is interesting that proline content alone is correlating to certain extent with protein adsorption on lignin surface (r^2 = 0.86). Prolines are generally abundant in flexible loop structures of proteins[34,35] as in the case of conalbumin (**Figure 6** and **Figure SI8**), and especially in the lignin binding random coil casein[36]. It is also known that these residues interact with phenolic compounds[37] and aromatic rings, likely *via* CH-π type polar interaction[25,26]. Prolines are also known to commonly participate in intermolecular interactions of proteins[25]. Further investigation of proline interactions is presented in the following section.

Another significant correlation was found to the number of hydroxyl bearing amino acids (r^2 = 0.89). This finding, in turn, is in agreement with the general protein adsorption model on hydrated surfaces, where the initial anchoring interaction has been proposed to be hydrogen bonding[22]. Hydroxyl containing residues tend to appear on the surfaces of globular proteins (**Figure SI5**), thus allowing extensive hydrogen bonding to take place, as indicated by the correlation data shown in **Table 2**.

Analysis of amino acid interactions with CLP. Different analytical techniques were used to gain further evidence regarding different types of amino acid – lignin interactions driving protein corona formation on CLP. First capillary electrophoresis (CE) was used to analyze phenylalanine, serine, proline, and valine interactions with the CLPs. Capillary electrophoretic mobilities of the selected amino acids in sole sodium benzoate solution and in the presence of CLPs are shown in **Figure 7**. As discussed in the previous section, clear signs of interaction could be detected in the case of serine, indicating to occurrence of hydrogen bonding with CLPs. Quite surprisingly, the electrophoretic mobility of phenylalanine and valine was not affected as strongly by the presence of CLPs, which is in contradiction with the apparent role of hydrophobic interactions. Instead, it is in a good agreement with the low correlation between hydrophobic residues alone and protein adsorption. In agreement with the observed correlation between proline content and protein adsorption, a significant reduction of the electrophoretic mobility of proline in the presence of CLPs was detected. Anyhow, the mobility of proline was low overall, raising some uncertainty about this result.

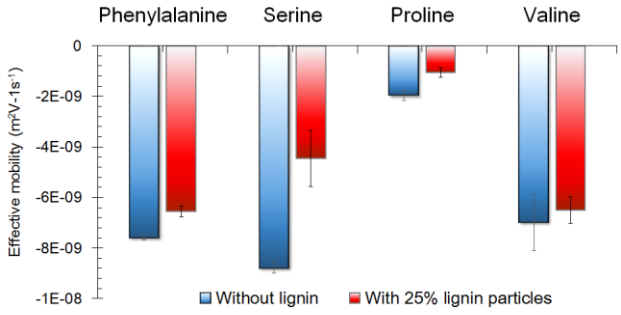

Figure 7. Interaction between different amino acid residues and CLPs as indicated by the reduction in electrophoretic mobility determined by capillary electrophoresis.

Further investigation of the plausible proline-lignin interaction was performed by FTIR-spectroscopy. The poly-L-proline was mixed either with epicatechin, a small lignin model compound, or with CLPs, followed by freeze drying of the samples. FTIR-spectra of the mixtures suggest interaction between phenolic moieties and poly-L-proline, with pronounced effects visible in the epicatechin spectra (**Figure SI9**). Weaker effects were observed with CLPs, as interactions were limited only to the surface of the particles. Clear band shifts detected in the FTIR spectra indicated the following types of intermolecular interactions: 1) Hydrogen bonding, likely between the carbonyl groups of the peptide backbone and hydroxyl groups of catechin or lignin. 2) CH-π type interactions between aromatic moieties of the phenol, and $-CH_2-$ of the proline ring in the peptide. These results are consistent with the finding about proline participitation in adsorption of protein and peptide onto lignin surfaces.

Important protein characteristics affecting adsorption to lignin on basis of this study.

Besides demonstrating a new concept of modifying the surface chemistry of colloidal lignin particles with proteins, we were able to point out the major interaction mechanisms that lead to pronounced corona formation. Fold structure of protein was found to be most influential on protein adsorption, as favorable interactions with the surface could take place more extensively in the case of random coil proteins. Favorability of Coulombic interactions was found to be the main driving force for protein adsorption in low ionic strength media, as long range repulsion forces could prevent anchoring of the protein to the lignin surface. In high ionic strength medium where Coulombic interactions were majorly screened off, a flexible coil structure of proteins allowed extensive short range polar interactions to take place, including hydrogen bonding, hydrophobic interactions, and possible CH-π interactions. The summary of our findings implemented in an analogous protein adsorption process, proposed by Penna et al. (2014)[22], are presented in **Scheme 1**.

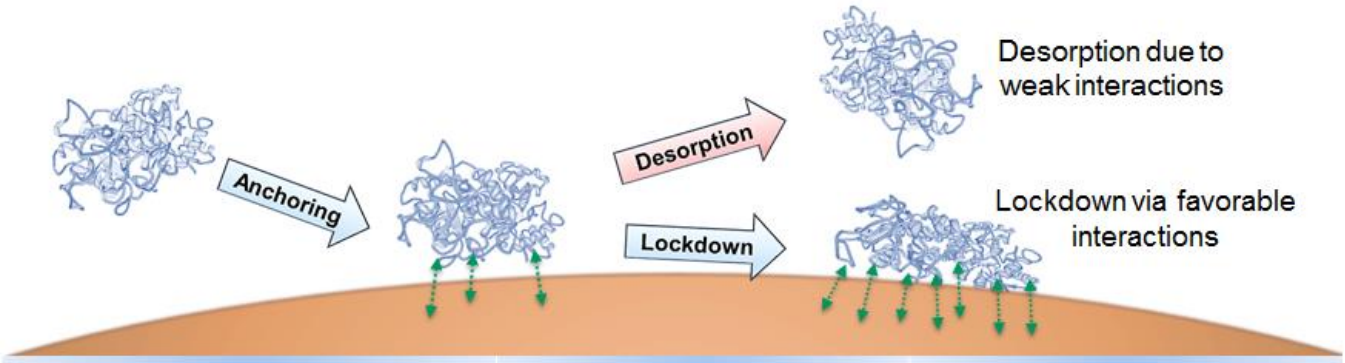

Property of protein	High adsorption	Low adsorption
Anchoring phase		
pI (in non-ionic medium)	**High** (positive charge)	**Low** (negative charge)
Number of OH-bearing residues	**High**	**Low**
Lockdown phase		
Fold structure	**Random coil**	**Globular**
Number of disulphide bridges	**Low**	**High**
Hydrophobicity	**Hydrophobic**	**Hydrophilic**
Number of proline residues *	**High**	**Low**

*Reflecting high number of flexible loops or interactions between the residue and lignin.

Scheme 1. Schematic illustration of protein adsorption on CLP surface and summary of the factors affecting protein adsorption on lignin surfaces.

Conclusions

In this study a facile method to prepare protein corona on CLPs using self-assembly was demonstrated. Such technology allows tailoring of functionality and surface charge of the lignin particles to meet requirements of the potential applications. Our results with actual CLPs and highly analogous model substrates could point out the main interaction mechanisms that drive protein corona formation on CLPs, with eminent influence arising from the adsorption medium.

The 3D fold structure of the protein was found to be most crucial single factor for efficient protein corona formation. Random coil proteins adsorbed over 2-fold better on surface of lignin nanoparticles than globular ones, demonstrating the importance of proteins ability to unfold and adjust its conformation during the adsorption process. This phenomenon was reflected also by the inverse correlation between cysteine content and protein adsorption.

The amino acid composition of the proteins determined the type and relative contributions of interactions with the lignin surface. While Coulombic forces predominated adsorption in non-ionic medium, polar type interactions, such as hydrogen bonding, and hydrophobic force were mainly driving the protein adsorption on lignin surface in high ionic strength media. Unexpectedly large amount of proline residues (typically associated to loop regions of the proteins) assisted protein corona formation on CLPs while details about participation of these residues on intermolecular interactions remained to be explored.

The understanding of the protein adsorption process allows screening of potential candidates from various data bases that could be exploited to form stabile protein corona on CLP for medical applications. Thus, the next step of our research will focus on interactions of coated CLPs with various tissue models. The most abundant proteins in skin and tissues include collagen and elastin, possessing most of the physicochemical properties found beneficial for protein–CLP interactions. Potential high volume applications of nanosized protein coated CLPs include different nanocomposites, wood adhesives, organic fillers in packaging, and edible food coatings. As such our study paves way for a vast number of future studies and applications of CLPs to be discovered.

ASSOCIATED CONTENT

Supporting Information. AFM-analysis and water contact angles of used model films. Amino acid compositions of used proteins. QCM-D analysis of protein adsorption in the case of varying adsorption media and film surface composition. Characterization of serum protein and poly-L-lysine coated CLPs. QCM-D data of protein adsorption on lignin films under varying ionic strength and use of poly-L-lysine as anchor. Hydrophobicity calculations and water contact angles of used model films. Structural images of conalbumin FTIR-data of poly-L-proline and epicatechin model mixtures. This material is available free of charge via the Internet at http://pubs.acs.org."

AUTHOR INFORMATION

Corresponding Author

* Tel. +358 40 770 9405; E-mail: timo.leskinen@aalto.fi

Author Contributions

The manuscript was written through contributions of Leskinen, Mattinen, and Österberg. Witos and Wiedmer contributed to work *via* CE-analysis, experimental design and data interpretation. Valle-Delgado contributed to the AFM-analyses and experimental design. Lintinen contributed to the TEM-analyses. All authors have given their approval to the final version of the manuscript.

FUNDING SOURCES

1. Aalto University (Espoo, Finland)
2. European Union (Bryssel, Belgium)
3. Academy of Finland (Helsinki, Finland)

ACKNOWLEDGEMENT

Aalto University (Espoo, Finland) are acknowledged for the financial support through the *Forest meets chemistry* -program and EU for the ZELCOR –project (*Zero Waste Ligno-Cellulosic Biorefineries by Integrated Lignin Valorisation*, #720303). M.-L. Mattinen and T. Leskinen acknowledges the Academy of Finland for the academy project (name, #276696), M. Österberg and J. J. Valle-Delgado for the research grant (name, #278279), and S.K. Wiedmer for the Academy of Finland research project (#266342). Magnus Ehrnrooth Foundation is also Acknowledged (S. K. Wiedmer). The study performed by Kalle Lintinen was carried out under the Academy of Finland's Centers of Excellence Programme (name, 2014-2019, #272361). The following persons are greatly appreciated for their work contribution: Jana Vanova and Emmi Mikkola (University of Helsinki, Helsinki, Finland) for CE-analyses. Marja Kärkkäinen and Rita Hatakka (Aalto University) are acknowledged for the laboratory assistance and Harry Boer (VTT) for assistance withMALDI-TOF analysis.

ABBREVIATIONS

AFM - Atomic force microscopy
BSA – Bovine serum albumin
CE – Capillary electrophoresis
CBM - Cellulose binding module
CLP - Colloidal lignin particle
DLS - Dynamic light scattering
PB – Phosphate buffer
PBS – Phosphate buffered saline
PDADMAC - Poly(diallyldimethylammonium chloride)
PE - Polyethylene
PS - Polystyrene
QCM-D - Quartz crystal microgravimetry with dissipation monitoring
TEM - Transmission electron microscopy

REFERENCES

1. Zhao, W.; Simmons, B.; Singh, S.; Ragauskas, A., & Cheng, G. *Green Chem*. **2016**, *18*, 5693-5700.
2. Fortunati, E.; Yang, W.; Luzi, F.; Kenny, J.; Torre, L.; Puglia, D. *Eur. Polym. J.* **2016**, *80*, 295-316.
3. Figueiredo, P.; Lintinen, K.; Kiriazis, A.; Hynninen, V.; Liu, Z.; Ramos, T. B.; Rahikkala, A.; Correia, A.; Kohout, T.; Sarmento, B.; Yli-Kauhaluoma, J.; Hirvonen, J.; Ikkala, O.; Kostiainen, M. A.; Santos, H. A. *Biomaterials* **2017**. *121*. 97-108.
4. Tortora, M.; Cavalieri, F.; Mosesso, P.; Ciaffardini, F.; Melone, F.; Crestini, C. *Biomacromolecules* **2014**, *15*, 1634-1643.
5. Carvalho, I. T.; Estevinho. B. N.; Santos. L. *Int. J. Cosmet. Sci.* **2015**, *38*, 109-119.
6. Appel, E. A.; Tibbitt, M. W.; Webber, M. J.; Mattix, B. A.; Veiseh, O.; Langer, R. *Nat. Commun.* **2015**, *6:6295*
7. Rose, S.; Prevoteau, A.; Elzière, P.; Hourdet, D.; Marcellan, A.; Leibler, L. *Nature* **2014**, *505*, 382-385.
8. Annabi, N.; Tamayol, A.; Shin, S. R.; Ghaemmaghami, A. M.; Peppas, N. A.; Khademhosseini, A. *Nano today* **2014**, *9*, 574-589.
9. Frangville, C.; Rutkevičius, M.; Richter, A. P.; Velev, O. D.; Stoyanov, S. D.; Paunov, V. N. *ChemPhysChem* **2012**, *13*, 4235-4243.
10. Qian, Y.; Deng, Y.; Qiu, X.; Li, H.; Yang, D. *Green Chem.* **2014**, *16*, 2156-2163.
11. Nypelö, T. E.; Carrillo, C. A.; Rojas, O. J. *Soft Matter* **2015**, *11*, 2046-2054.
12. Lievonen, M.; Valle-Delgado, J. J.; Mattinen, M-L.; Hult, E. L.; Lintinen, K.; Kostiainen, M. A.; Paananen, A.; Szilvay, G. R.; Setälä, H.; Österberg, M. *Green Chem*. **2016**, *18*, 1416-1422.
13. Li, H.; Deng, Y.; Wu, H.; Ren, Y.; Qiu, X.; Zheng, D.; Li, C. *Holzforschung* **2016**, *70*, 725–731
14. Richter, A. P.; Bharti, B.; Armstrong, H. B.; Brown, J. S.; Plemmons, D. A.; Paunov, V. N.; Stoyanov, S. D.; Velev, O. D. *Langmuir* **2016**, *32*,6468–6477
15. Jiang, C.; He, H.; Jiang, H.; Ma, L.; Jia, D. M. eXPRESS Polym. Lett. **2013**, 7(5).
16. Palonen, H.; Tjerneld. F.; Zacchi, G.; Tenkanen, M. *J. Biotechnol*. **2004**, *107*, 65-72.
17. Salas, C.; Rojas, O. J.; Lucia, L. A.; Hubbe, M. A.; Genzer, J. *ACS Appl. Mater. Interfaces* **2012**, *5*, 199-206.

18. Rahikainen, J. Cellulase-lignin interactions in the enzymatic hydrolysis of lignocellulose. VTT Technical Research Centre of Finland, Espoo, Finland, **2013**
19. Strobel, K. L.; Pfeiffer, K. A.; Blanch, H. W.; Clark, D. S. *J. Biol. Chem.* **2015**, *290*, 22818-22826.
20. Yamaguchi, A.; Isozaki, K.; Nakamura, M.; Takaya, H.; Watanabe, T. *Sci. Rep.* **2016***, 6,* 21833.
21. Vogler, E. A. *Biomaterials* **2012**, *33*, 1201-1237.
22. Penna, M. J.; Mijajlovic, M.; Biggs, M. J. *J. Am. Chem. Soc.* **2014**, *136*, 5323-5331.
23. Mizutani, K.; Mikami, B.; Aibara, S.; Hirose, M. Acta Crystallogr.. Sect. D: Biol. Crystallogr. 2005. 61(12). 1636-1642.
24. Pettersen, E. F.; Goddard, T. D.; Huang, C. C.; Couch, G. S.; Greenblatt, D.M.; Meng, E.C.; Ferrin, T. E. J Comput Chem. 2004, 25, 1605-1612.
25. Bhattacharyya, R.; Chakrabarti, P. *J. Mol. Biol.* **2003**, *331*, 925-940.
26. Nishio, M.; Umezawa, Y.; Fantini, J.; Weiss, M. S.; Chakrabarti, P. *Phys. Chem. Chem. Phys.* **2014**, *16*, 12648-12683.
27. Tammelin, T.; Österberg, M.; Johansson, L.-S.; Laine, J. *Nord. Pulp Pap. Res. J.* **2006**, *21,* 444–450
28. Tenzer, S.; Docter, D.; Kuharev, J.; Musyanovych, A.; Fet, V.; Hecht, R.; Schlenk, F.; Fischer, D.; Kiouptsi, K.; Reinhardt, R.; Landfester, K.; Schild, H.; Maskos, M.; Knauer, S. K.; Stauber, R. H. *Nat. Nanotechnol.* **2013**, *8*, 772-781.
29. Norde, W. *Colloids Surf. B* **2008**, *61*, 1-9.
30. Fass, D. *Annu. Rev. Biophys.* **2012**, *41*, 63-79.
31. Dobrynin, A. V.; Colby, R. H.; Rubinstein, M. *J. Polym. Sci., Part B: Polym. Phys.*, **2004,** *42*, 3513-3538.
32. Vogler, E. A. *Adv. Colloid Interface Sci.* **1998**, *74*, 69-117.
33. Salgado, J. C.; Rapaport, I.; Asenjo, J. A. *J. Chromatogr. A* **2005**, *1098*, 44-54.
34. Williamson, M. P. *Biochem. J.* **1994**, *297*, 249.
35. Tompa, P. *Trends Biochem. Sci.* **2002**, *27*. 527-533.
36. Kumosinski, T. F.; Brown, E. M.; Farrell, H. M. *Journal of dairy science* **1993**, *76*, 931-945.
37. Charlton, A. J.; Baxter, N. J.; Lilley, T. H.; Haslam, E.; McDonald, C. J.; Williamson, M. P. *FEBS let.* **1996**, *382*, 289-292.

Table of Contents Graphic

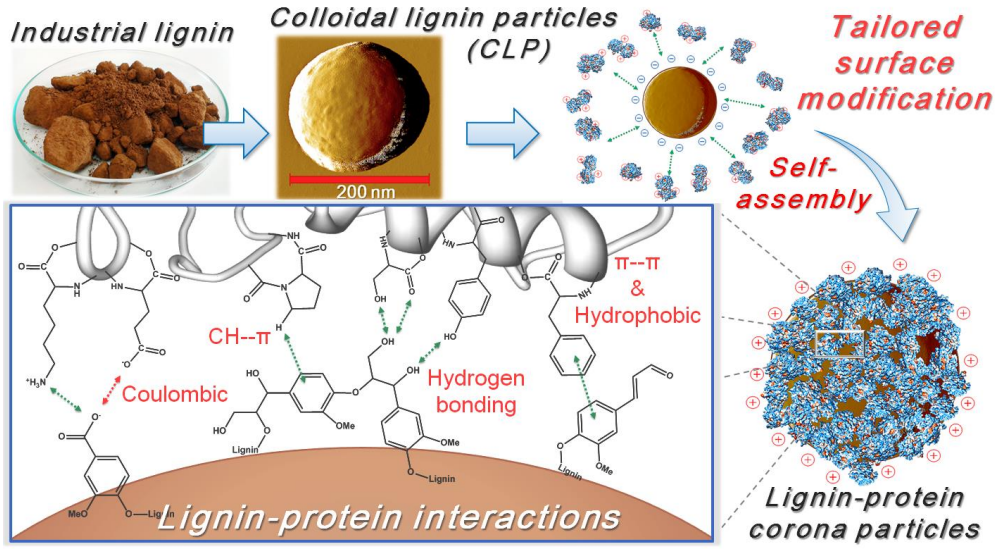

Supporting information

Adsorption-driven assembly of protein on colloidal lignin particles for advanced biomaterials

Timo Leskinen, Joanna Witos, Juan José Valle-Delgado, Kalle Lintinen, Mauri Kostiainen, Susanne K. Wiedmer, Monika Österberg, and Maija-Liisa Mattinen

SI1 - Water contact angle of lignin thin films

Table SI1 Water contact angles on QCM crystals with and without coating

Type of surface	**Gold**	**Polystyrene**	**Lignin**
Determined contact angle θ (°)	59 ± 10	68 ± 1	52 ± 7

SI2 - Atomic force microscopy (AFM) analysis of lignin thin films

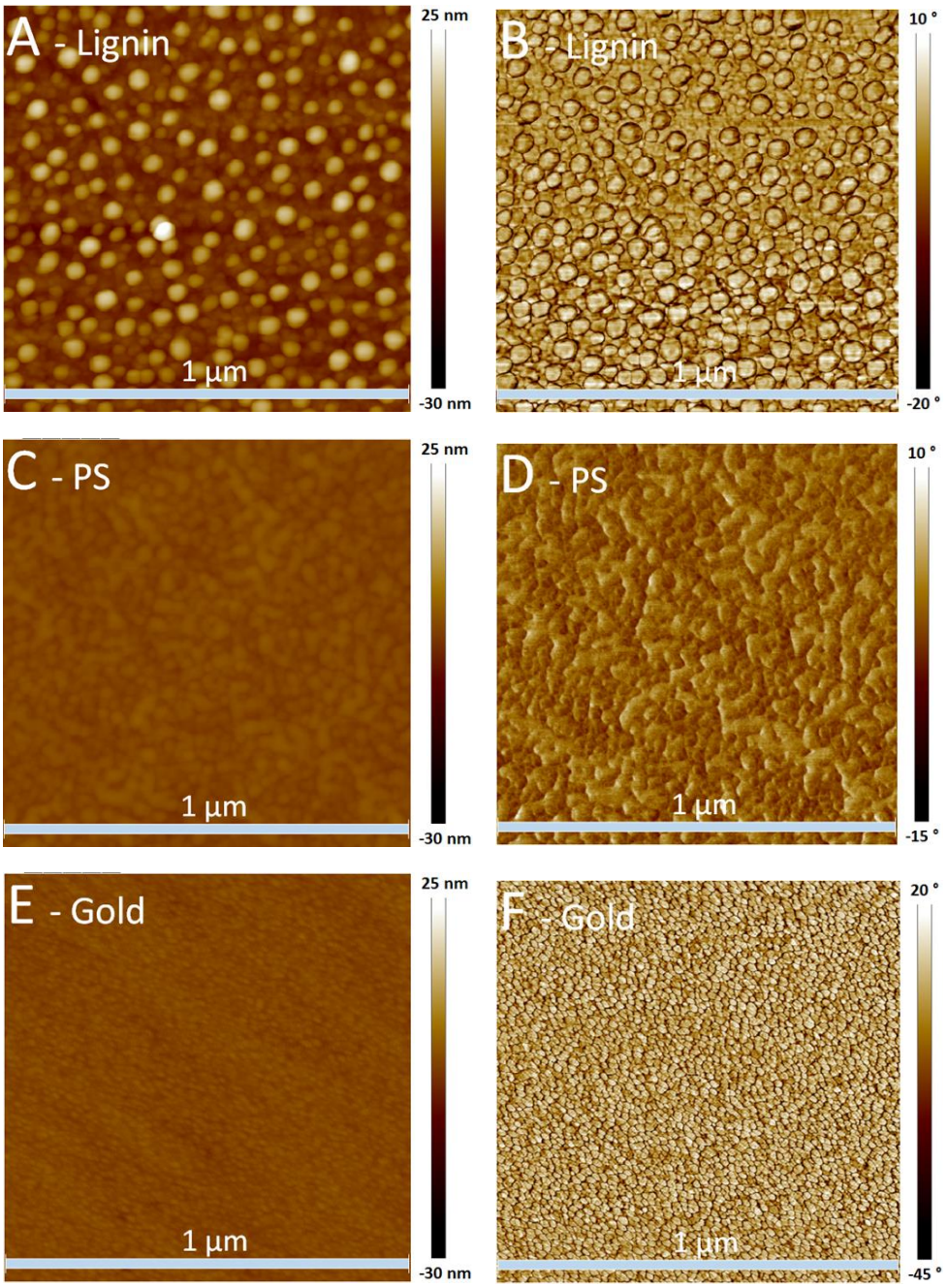

Figure SI1. AFM height and phase images from used lignin thin films on QCM crystals **(A & B)**, PS pre-coated QCM crystals **(C & D)**, and bare gold QCM crystals **(E & F)**. AFM measurements were done in tapping mode in air as described by Valle-Delgado et al. (2016), with exception that NCHV-A tapping mode probes from Bruker were used. (Valle-Delgado, J. J.; Johansson, L. S.; Österberg, *M. Colloids Surf. B,* **2016**, *138,* 86-93.)

SI3 - Amino acid compositions of analyzed proteins

Amino acid compositions were calculated as mass percentages, based on the following literature. Molar ratios found in some sources were first converted to corresponding mass for such purposes.

BSA

Lewis, J. C.; Snell, N. S.; Hirschmann, D. J.; Fraenkel-Conrat, H. *J. Biol. Chem.* **1950**, *186*, 23-35.

Stein, W. H.; Moore, S. In *Cold Spring Harbor symposia on quantitative biology*, Cold Spring Harbor Laboratory Press. 1950, p.179-190

Peters, T. *Clin. Chem.* **1968**, *14*, 1147-1159.

Conalbumin

Lewis, J. C.; Snell, N. S.; Hirschmann, D. J.; Fraenkel-Conrat, H. *J. Biol. Chem.* **1950** 186, 23-35.

Williams, J. *Biochem. J.* **1962** *83*, 355.

Azari, P.; Baugh, R. F. *Arch. Biochem. Biophys.* **1962**, *118*, 138-144.

Casein

Lauer, B. H.; Baker, B. E. *Can. J. Zool.* **1977**, *55*, 231-236.

Rutherfurd, S.; Moughan, P. *J. Dairy Sci.* **1998**, *81*, 909-917.

Gelatin

Farris, S.; Song, J.; Huang, Q. *J. Agric. Food Chem.* **2009** *58*, 998-1003.

Eastoe, J. E. *Biochem. J.* **1955**, *61*, 589.

Wu, C. K.; Tsai, J. S.; Chen, Z. Y.; Sung, W. C. *Food Sci. Technol. Int.* **2015** *21*, 284-294.

SI4 - Analyzes of corona particles

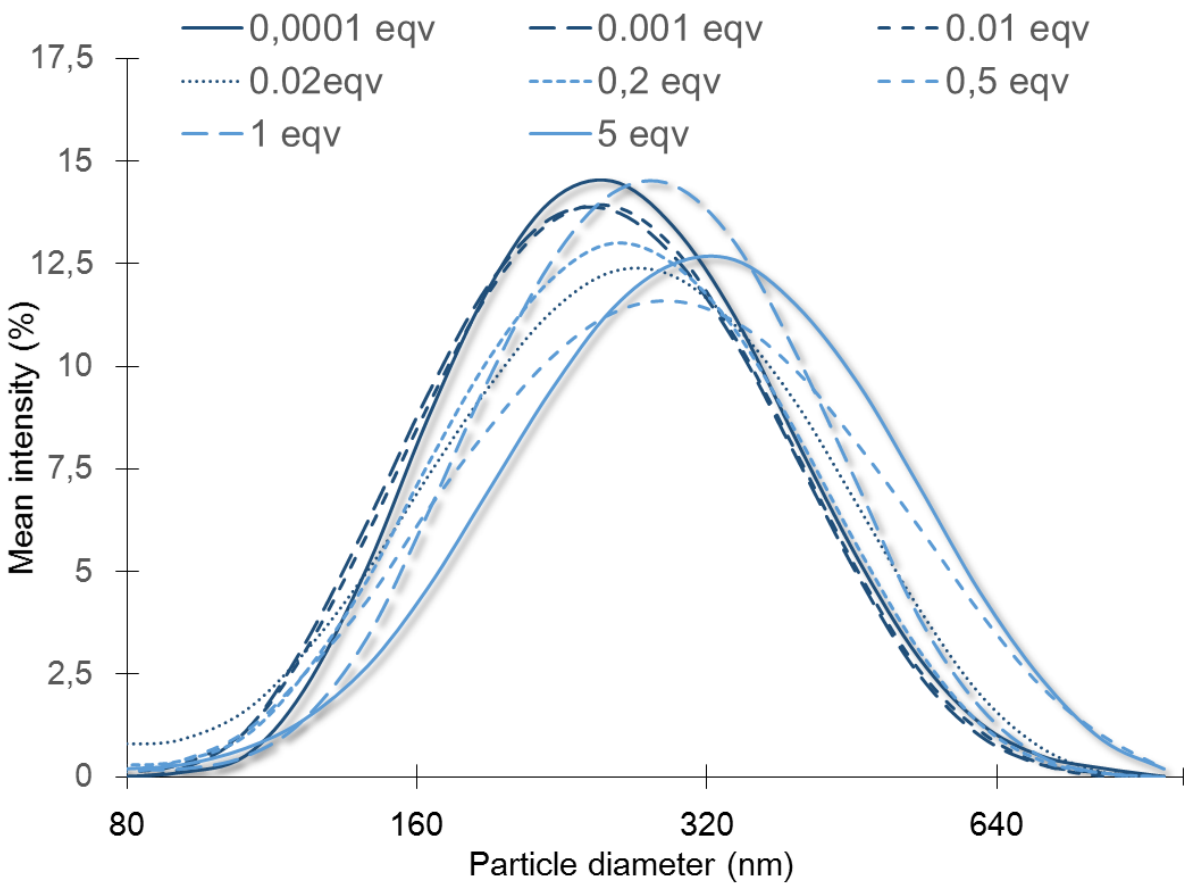

Figure SI2. Particle size distributions of poly- L-lysine samples presented in Figure 1B, showing the overall shift of the whole distribution, and lack of aggregates consisted of multiple CLPs.

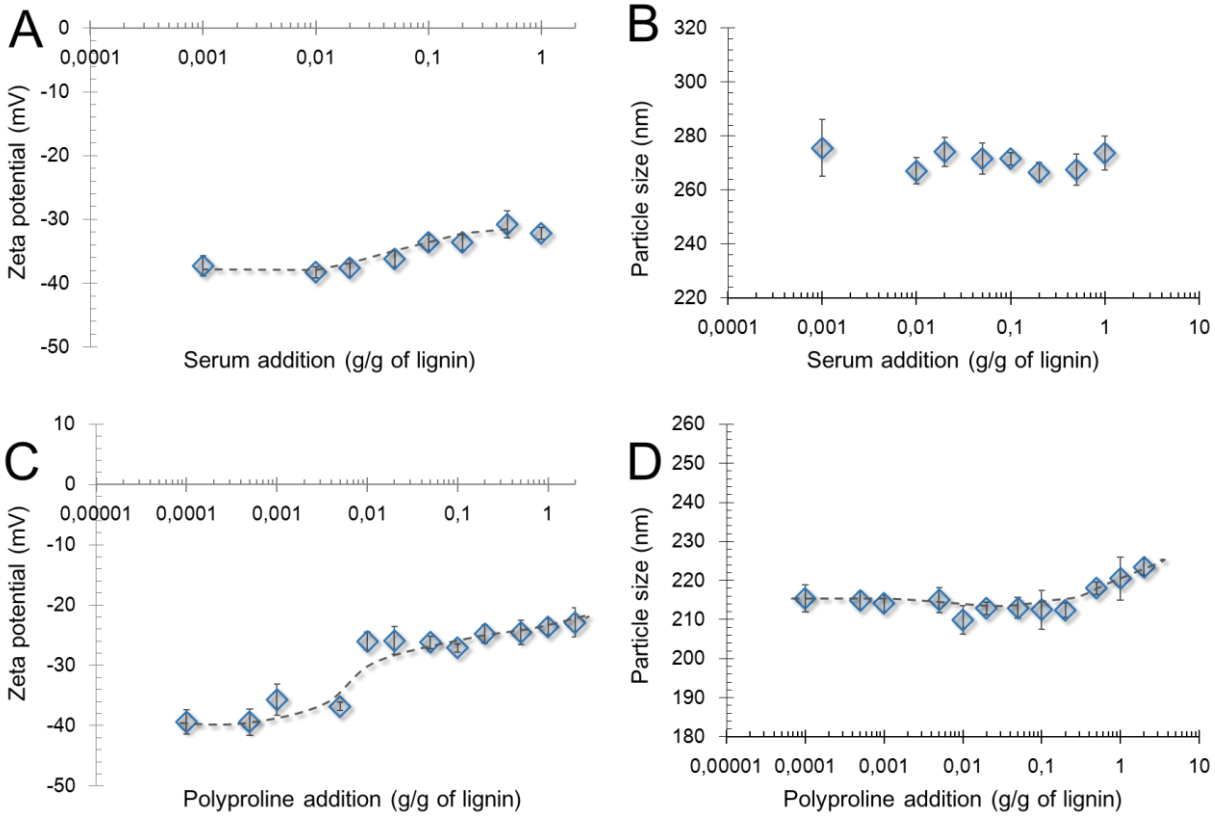

Figure SI3. Zeta potential and particle sizes of lignin nanoparticles after coating with serum proteins **(A & B)** or poly- L-proline **(C & D)**.

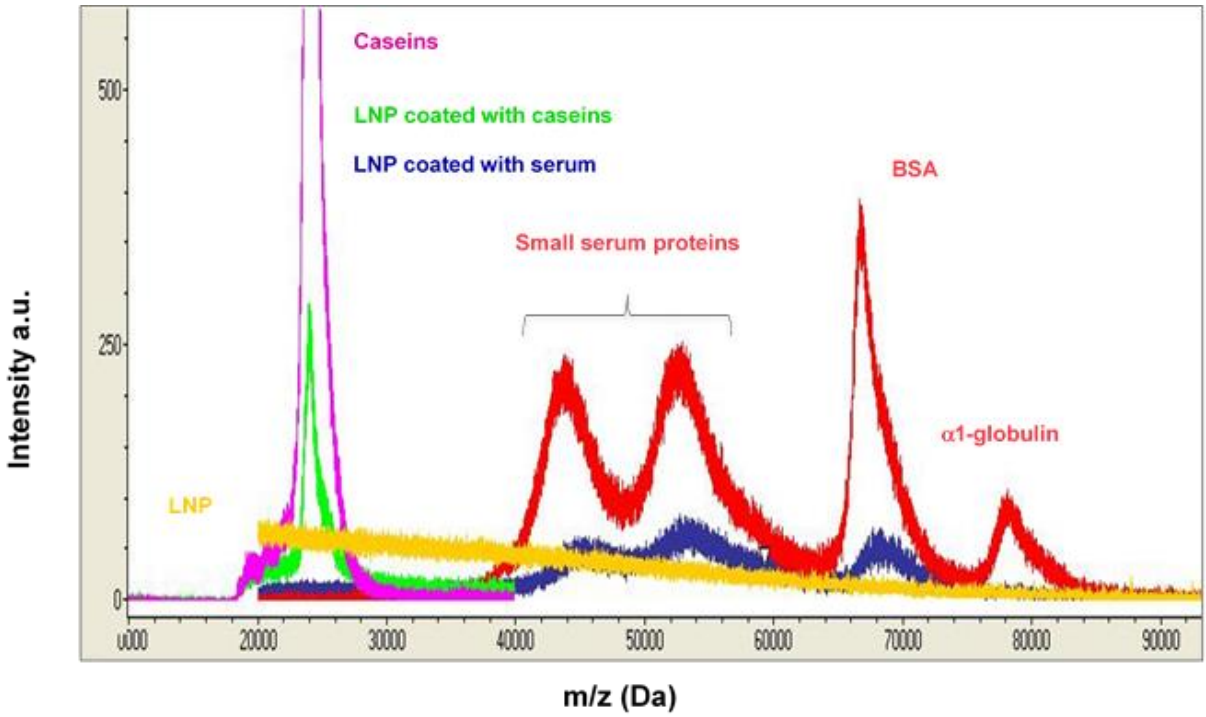

Figure SI4. Coating CLPs with proteins as evidenced by MALDI-TOF MS. Proteins were adsorbed on CLPs followed by solvent exchange and removal of free proteins using filtration. One weight eqv. of protein was used for CLP coating. Adsorption of different proteins was evident from MALDI-TOF MS spectrum and zeta potential measurements.

Matrix assisted laser desorption ionization-time-of-flight mass spectrometry (MALDI-TOF MS) experimental. CLPs were coated with proteins as described and excess of proteins was removed by repeated exchange of water using Vivaspin-centrifugal concentrator tubes. Purified CLP dispersions containing protein coated particles were dried on target plate together with a saturated solution of sinapinic acid matrix compound in 0.1% trifluoroacetic acid (TFA)-acetonitrile mixture. Spots were let to dry onto target plate in fume hood. The analysis was conducted using a mass spectrometer (Bruker AutoflexII, Germany).

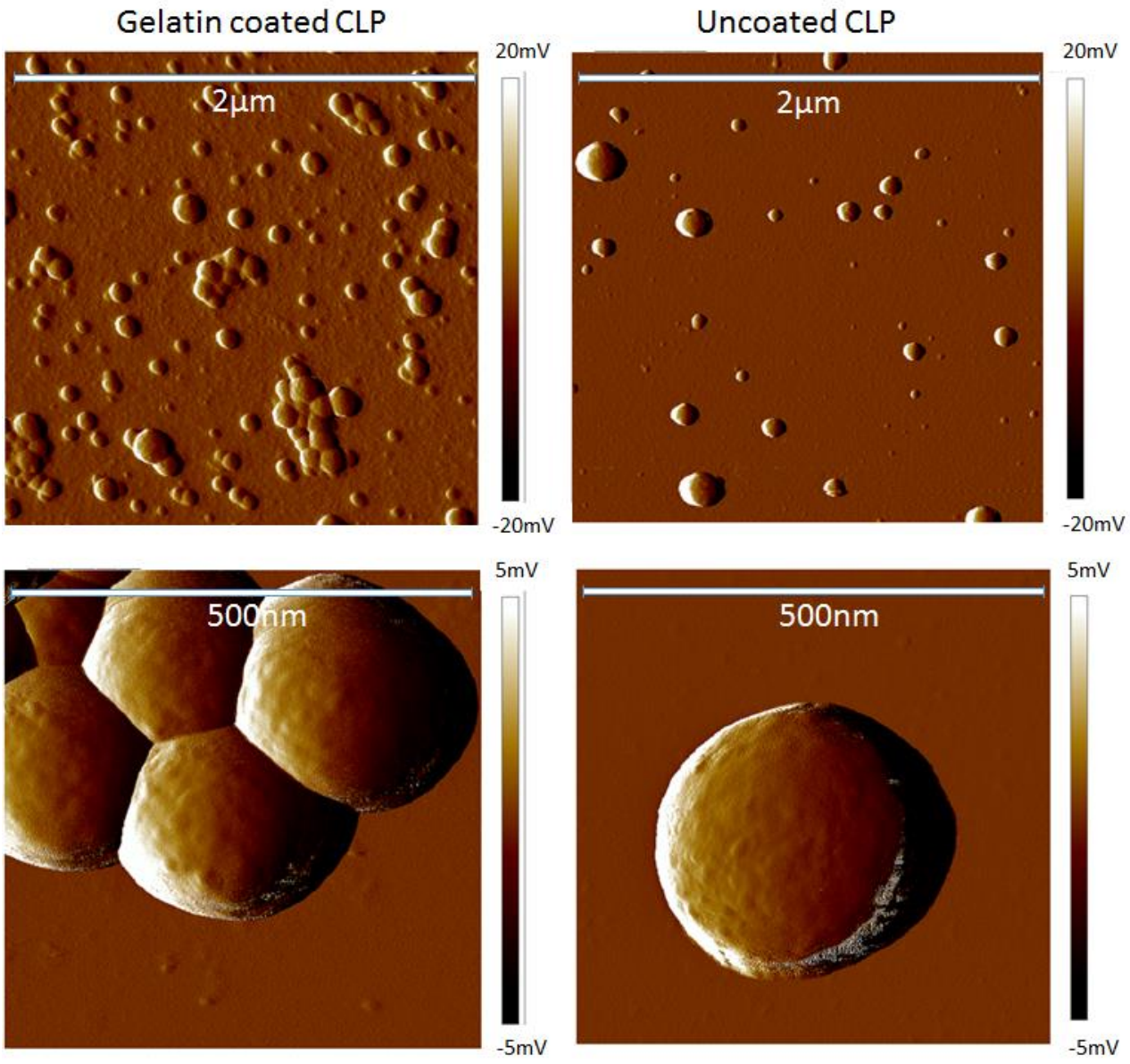

Figure SI5. AFM amplitude error images of gelatin coated CLPs (left up and left down) and uncoated CLPs (right up and right down).

SI5 - Effect of ionic strength of adsorption medium

Table SI2 Adsorption of model proteins on lignin thin film from various media with differing ionic strength, measured as frequency change of QCM-crystal.

Model protein		***Vibration change upon protein adsorption - Δf5 (Hz)***		
		Lignin thin film		
	pI	PBS (180 mM; pH 7.4)	PB (25 mM; pH 7.4)	Water (0 mM; pH > 6.4)
Albumin	4.6 – 5.8	8	2	2
Casein	4.1 – 5.8	44	34	-
Casein (sodium salt)		-	-	3
Conalbumin	6.8	20	25	36
Gelatin	7.0 – 9.0	45	52	111

Table SI3 Adsorption of tested proteins on lignin, polystyrene (PS), and polyethylene (PE) films from various media with differing ionic strength, measured as frequency change of QCM-crystal. See table SI3 for ionic strength of used buffers.

Model protein	***Vibration change upon protein adsorption - Δf5 (Hz)***					
	Lignin			**PS**		**PE**
	PBS	PB	Water	PBS	PB	PBS
Albumin	8	2	2	11	4	8
Casein	44	34	-	43	36	-
Casein (sodium salt)	-	-	3	-	-	39
Conalbumin	20	25	36	26	24	8
Gelatin	45	52	111	51	72	26

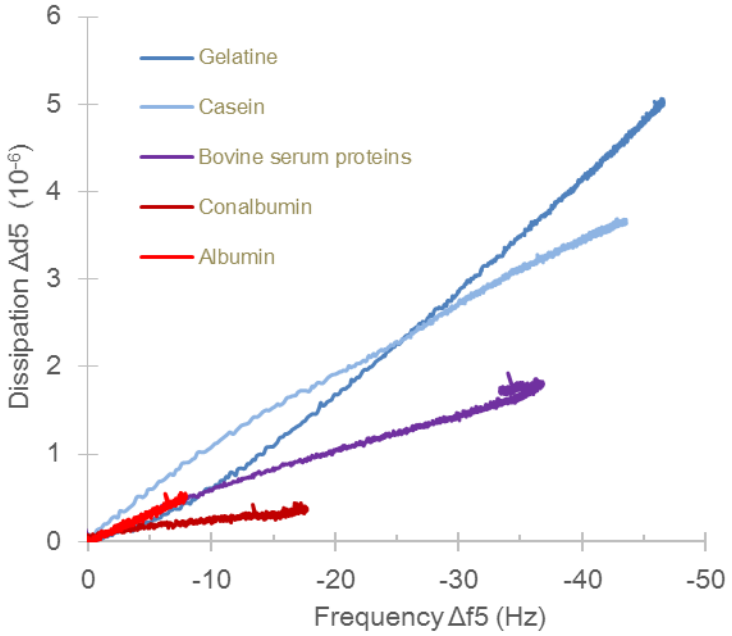

Figure SI6. Dissipation against frequency changes during adsorption of model proteins on lignin films in PBS buffer.

SI5 – Adsorption of protein layer via poly- L-lysine anchor

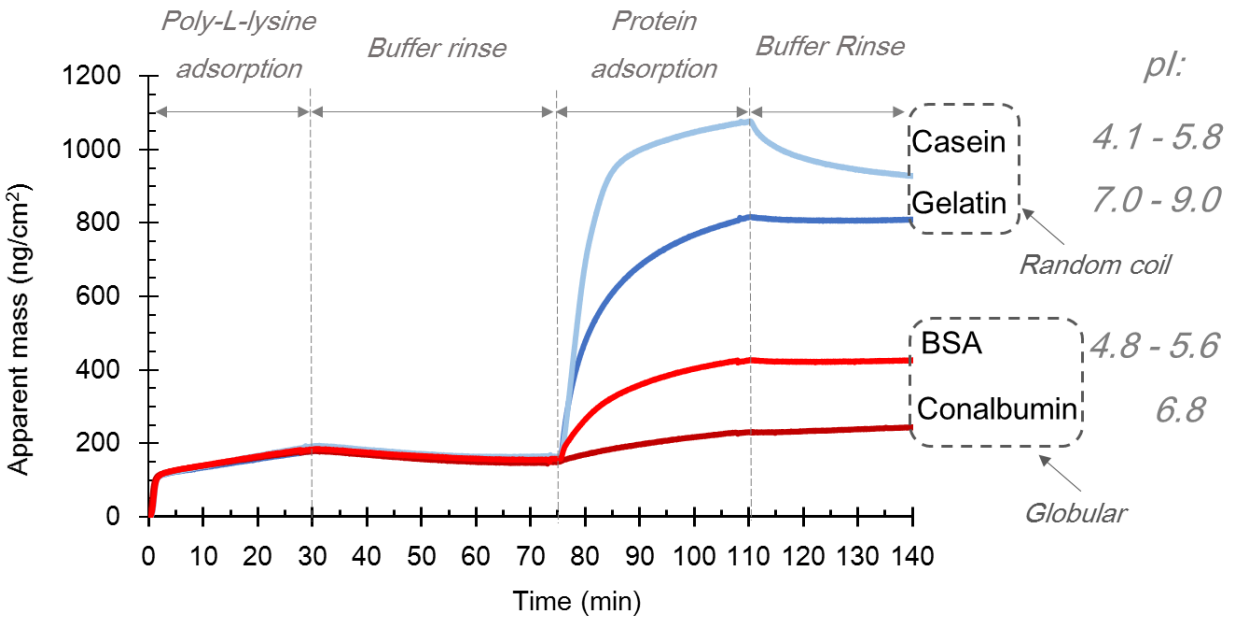

	Albumin	Conalbumin	Casein	Gelatin
Average adsorption (ng/cm2)	270	82	911	668
Change to lignin surface	+ 43 %	-78 %	+ 11 %	-24 %

Figure SI7. Influence of poly-L-lysine pre-coating the adsorption of model proteins on lignin thin films as analyzed by QCM-D in PBS buffer solution with ionic strength of 180 mM.

SI6 - Estimation of relative hydrophobicity for lignin, PS, and PE films using Hansen solubility parameter calculations

1) $R_a^2 = 4(\delta_{D1} - \delta_{D2})^2 + (\delta_{P1} - \delta_{P2})^2 + (\delta_{H1} - \delta_{H2})^2$

2) $RED = \frac{R_a}{R_0}$

According to theory by Hansen (1967), RED-values below one indicate favorable dispersion/solubility of polymer in a solvent. RED-values above one are typical for phase separating compounds.

Hansen, C. M. (1967). The Three Dimensional Solubility Parameter and Solvent Diffusion Coefficient - Their Importance in Surface Coating Formulation, Danish Technical Press, Copenhagen

Table SI1 Calculated RED-values between water and film materials, indicating the relative hydrophobicity between these materials. REW > 1 means a clearly hydrophobic surface.

Material	δ_d	δ_p	δ_h	R_0	$RED_{water\text{-}polymer\ film}$
Water	18,1	17,1	16,9	13,0	-
Lignin	21,9	14,1	16,9	13,7	0,63
Polystyrene	21,3	5,8	4,3	12,7	1,39
Polyethylene	16,3	5,9	4,1	8,2	1,34

SI8 – Locations of amino acid residues within fold structure of conalbumin

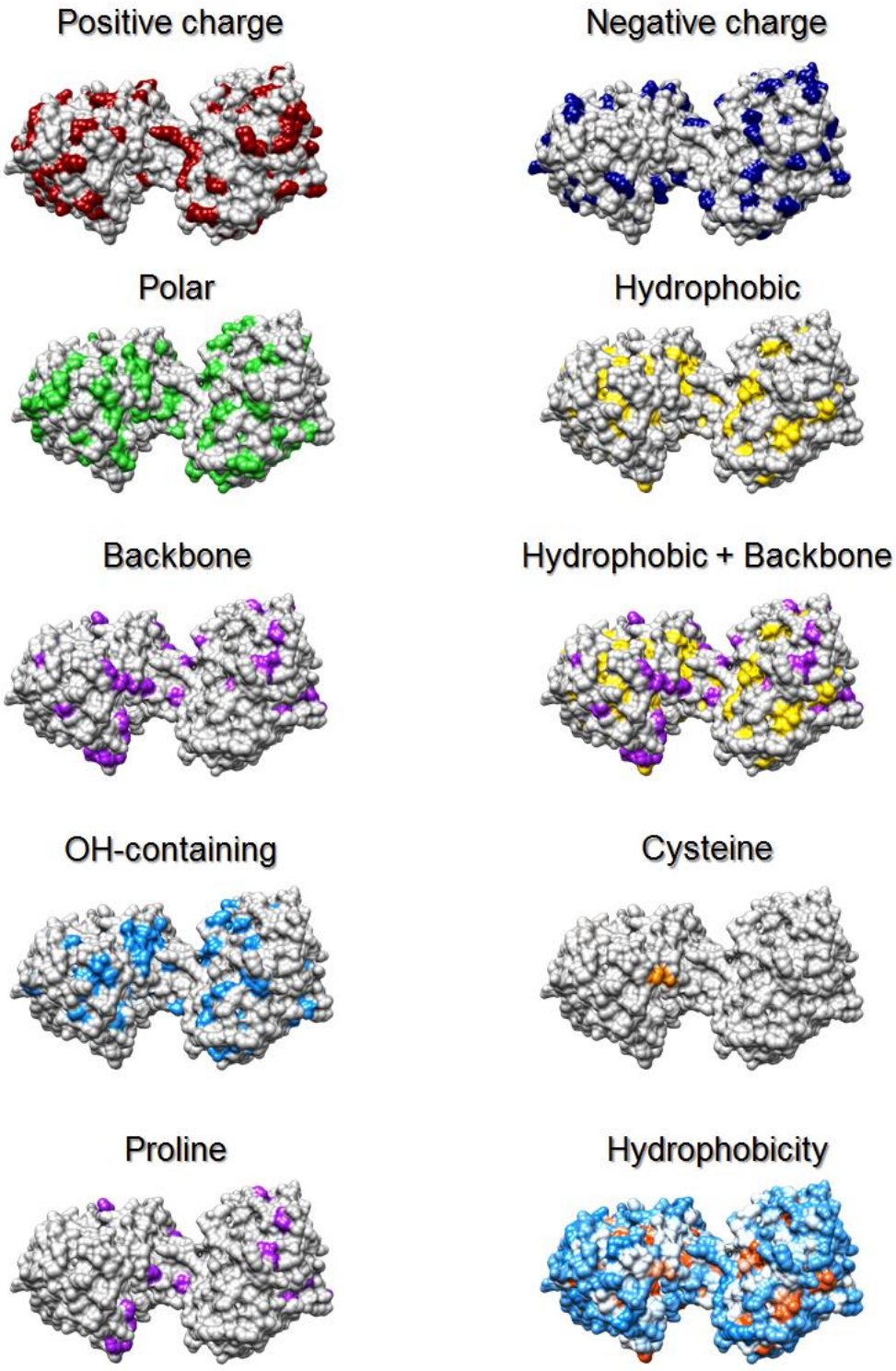

Figure SI8. Locations of amino acid residues listed in **Table 2** within structure of Conalbumin (PDB ID: 2D3I) surface as calculated by Chimera™ software.

SI9 – FTIR-analysis of poly- L-proline interaction with epicatechin

A

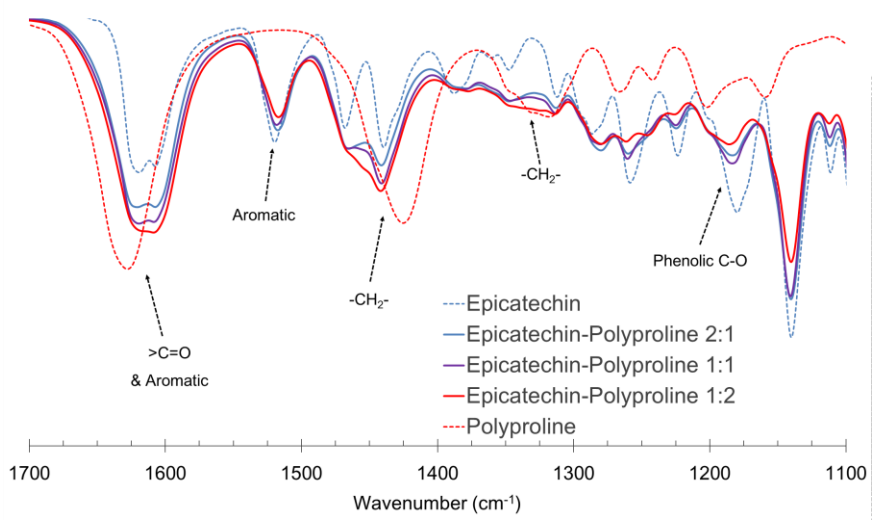

B

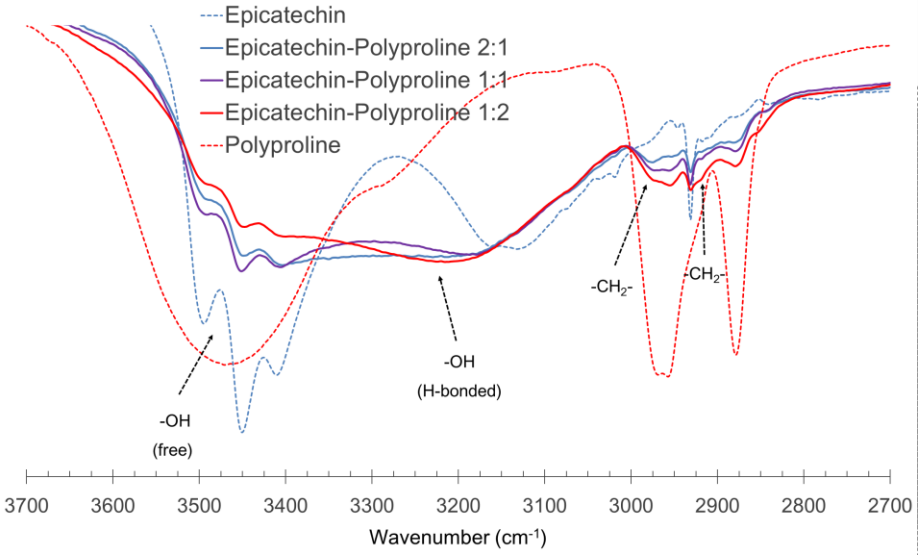

Figure SI9. FTIR-spectra recorded in order to identify interactions between poly- L-proline and epicatechin phenolic model compound. Bands with shifting, broadening, or significant decrease in intensity are marked in the spectra with assignments**. (A)** 1700 – 1100 cm^{-1} region **(B)** 3700 – 2700 cm^{-1} region.